

Original Research

Differential Response to Cisplatin between Co-cultured Cells and Pure Cultured Cells Based on Single-cell RNA Sequencing of Three-dimensional-cultured Breast Cancer Cells

Shuqing Yang^{1,2,†}, Peixian Chen^{1,†}, Xiaofan Mao³, KaiRong Lin³, Wei Li¹, Tiancheng He¹, Huiqi Huang¹, AiGuo Wu⁴, Wei Luo³, Guolin Ye¹, Guangyu Yao^{2,*}, Dan Zhou^{1,*}

Academic Editor: Amancio Carnero Moya

Submitted: 9 May 2024 Revised: 3 July 2024 Accepted: 23 September 2024 Published: 29 November 2024

Abstract

Objective: The current study aimed to develop an experimental approach for the direct co-culture of three-dimensional breast cancer cells using single-cell RNA sequencing (scRNA-seq). Methods: The following four cell culture groups were established in the Matrigel matrix: the untreated Michigan Cancer Foundation (MCF)-7 cell culture group, the MCF-7 cell culture plus cisplatin group, the untreated co-culture group, and the cell co-culture plus cisplatin group. For cell co-culture, MCF-7 cells, human mammary fibroblasts, and human umbilical vein endothelial cells were mixed at a ratio of 1:1:1. Cisplatin was applied at a concentration of 1.25 μg/mL, and the cells were harvested after 2 days and subjected to scRNA-seq. Data were analyzed using a single-cell RNA sequencing data analysis pipeline with R language. Results: The response of MCF-7 cells to cisplatin differed among the four groups. The transcriptomic response of MCF-7 cells to cisplatin in the co-culture model was not as significant as that in the mono-culture model. Moreover, the pathways related to apoptosis, DNA damage, hypoxia, and metastasis in the co-culture groups were enriched in the genes that were differentially expressed based on cisplatin treatment. Conclusion: scRNA-seq analysis revealed that the response of MCF-7 cells to cisplatin in the co-culture model was lower than that in the mono-culture model. Therefore, the three-dimensional cell co-culture model can be applied to tumor research to better mimic the pathophysiological environment *in vivo* and can be a well-modified research method.

Keywords: three-dimensional cell coculture; single-cell RNA sequencing; MCF-7 cells; breast cancer

1. Introduction

Laboratory tumor modeling is essential to improve the understanding of tumor biology and to develop novel treatment strategies for breast cancer. Cell-based tumor experiments are ubiquitous in cancer research. However, traditional two-dimensional (2D) cell line experiments cannot reproduce the complexity of *in vivo* tumors. Cell co-culture experiments (e.g., those using the Transwell incubator) can be used to assess cell interactions. However, these cell coculture approaches involve communication between extracellular vesicles and other factors, not direct contact between cells [1,2]. Researchers have developed methods for the three-dimensional (3D) culture of cancer cells. These models can better mimic the biological behavior of in vivo tumors than traditional culture methods [3,4], particularly in the co-cultures of multiple cell types, and can reproduce cell heterogeneity. Therefore, 3D culture can better reflect the actual condition of tumors than 2D culture [5]. The application of 3D breast cancer cell culture, particularly in drug resistance mechanisms and individualized therapy, has been

comprehensively evaluated. Tatara et al. [6] showed that compared with 2D culture, 3D culture is more effective in simulating trastuzumab-induced apoptosis and the cytological and biochemical mechanisms of trastuzumab resistance associated with phosphatidylinositol-4, 5-bisphosphate 3kinase catalytic subunit alpha (PIK3CA) mutations. Lugert et al. [7] developed Ptx functionalized superparamagnetic iron oxide nanoparticles coated with lauric acid and human serum albumin. Moreover, their efficacy in different breast cancer cell lines in 2D and 3D cultures was examined [7]. Fuzer et al. [8] analyzed and compared the anticancer activity of [9] gingerol in breast cancer HMT-3522 cells grown in 3D culture lr-extracellular matrix and non-malignant S1 cells [9]. Gingerol enhances the cytotoxicity of linear HMT-3522 (T4-2) cells and induces the apoptosis of breast cancer HMT-3522 (T4-2) cell line [8]. Meanwhile, singlecell RNA sequencing (scRNA-seq), a novel experimental method, has been increasingly used in basic and clinical tumor research [10]. Thus, direct cell co-culture can be performed, and different cells and functions at the single-cell level can be identified [9]. Cisplatin is effective against var-

 $^{^{1}}$ Department of Breast Surgery, The First People's Hospital of Foshan, 528100 Foshan, Guangdong, China

²Breast Center, Nanfang Hospital, Southern Medical University, 510515 Guangzhou, Guangdong, China

³Clinical Research Institute, The First People's Hospital of Foshan, 528100 Foshan, Guangdong, China

⁴Department of General Surgery, Zhujiang Hospital, Southern Medical University, 51000 Guangzhou, Guangdong, China

^{*}Correspondence: yaogy@smu.edu.cn (Guangyu Yao); zdan14@fsyyy.com (Dan Zhou)

[†]These authors contributed equally.

ious types of cancers including ovarian cancer, metastatic testicular cancer, bladder cancer, lung cancer, and breast cancer [11]. Cisplatin treatment alone has a lower cure rate in patients with breast cancer. Thus, it is commonly used in combined therapy for breast cancer. The current study used cisplatin as an intervention drug acting on cultured cells.

In the current experiment, Michigan Cancer Foundation (MCF)-7 cells, human mammary fibroblasts (HMFs), and human umbilical vein endothelial cells (HUVECs) were mixed for 3D culture and treated with cisplatin. Then, the transcriptional changes in MCF-7 cells were observed at the single-cell level. This study aimed to validate the superiority of scRNA-seq combined with 3D cell direct co-culture in breast cancer research. Results showed that scRNA-seq combined with 3D cell direct co-culture can be a promising *in vitro* cancer cell culture approach.

2. Methods

2.1 Three-dimensional in Vitro Cell Coculture

MCF-7 cells (ZQ0071) and HUVECs (ZQ1099) were acquired from Shanghai Zhongqiao Xinzhou Biotechnology Co., Ltd. (Shanghai, China). HMFs (MZ-2683) were obtained from Ningbo Mingzhou Biotechnology Co., Ltd. (Ningbo, China). Cell lines were authenticated by the Genomics Unit, using ShortTandem Repeat profiling (AmpFLSTR® Identifier® Plus PCR Amplification Kit, Waltham, MA, USA). Mycoplasma test was perfored in all cell lines every other week using the lycoAlertMycoplasma Detection Kit (LONZA, Basel, Switzerland), The test results were negative. MCF-7 cells, HMFs, and HUVECs were mixed at a ratio of 1:1:1 [12] and then cultured in a previously prepared Matrigel matrix (356237, Corning Co., Shanghai, China) to construct a 3D co-culture model. In the MCF-7 cell 3D culture, only MCF-7 cells were added in the Matrigel matrix. For preparation, the Matrigel matrix was removed from -80 °C and placed in a 4 °C refrigerator for 2 h. Cells were collected and re-suspended in the Dulbecco's Modified Eagle Medium-high (DMEM-H) medium supplemented with 15% fetal bovine serum (FBS) and mixed with the Matrigel matrix together at a final concentration of 4.5 mg/mL for Matrigel and 6×10^6 /mL for cells. In total, 24 μL of 2.5 mmol cisplatin was added to each 2-mL medium for treatment. The final concentration was 1.25 mmol/mL. The experiment was performed on four groups, which were as follows: MCF-7 cells in the 3D culture, MCF-7 cells in the 3D culture treated with cisplatin, 3D co-culture model, and the 3D co-culture model with cisplatin. In each group, cells were harvested 2 days after cisplatin treatment and were subjected to scRNA-seq.

2.2 Single-cell Processing and Library Preparation

Using the Single Cell 3' Library and Gel Bead Kit V3 ($10 \times$ Genomics, 1000075, Pleasanton, CA, USA) and the Chrome Single Cell B Chip Kit ($10 \times$ Genomics, 1000074), cell suspensions (300-600 live cells per microliter as mea-

sured using Count Star) were loaded onto a chromium single-cell controller (10× Genomics). Single-cell gel beads were generated in the solution according to the BD RhapsodyTM Single-Cell Analysis System manual. Thus, single cells were suspended in phosphate-buffered saline containing 0.04% bovine serum albumin. The captured cells were cleaved, and the released RNA was barcoded by performing reverse transcription in a single GEM. Reverse transcription was performed on the S1000TM Touch Thermal Cycler (Bio Rad, Hercules, CA, USA) at 53 °C for 45 min and then at 85 °C for 5 min. Next, it was held at 4 °C. Finally, cDNA was generated. The final library was quantified using the Qubit fluorescence assay with the Qubit ds-DNA HS kit (Thermo Fisher, Carlsbad, CA, USA). The library was sequenced by Novogene Biotech Co., Ltd. (Beijing, China) on the NovaSeq 6000 in the paired-end mode.

Cells were revived and processed using BD Rhapsody single cell analysis system the BD Rhapsody Express Single-Cell Analysis System (BD Biosciences, Franklin Lake, NJ, USA), according to the manufacturer's instructions. Briefly, an average of 20,000–30,000 pooled cells was loaded in each cartridge on the BD Rhapsody express single cell analysis system for single cell capture, and the library was prepared using BDTM Single-Cell Multiplexing Kit-Human and BD Rhapsody Single Cell Multiplexing Kit as per manufacturer's guide (Doc ID: 214419 Rev. 2.0). Final libraries were quantified using Qubit and Agilent TapeStation and pooled to achieve a final concentration of 5 nM. The libraries were sequenced using NovaSeq 6000 by Novogene Biotech Co., Ltd. (Beijing, China).

2.3 Analysis of scRNA-seq Data

To control quality, cells expressing <300 or >6000genes were excluded. To eliminate dying cells or lowquality cells with extensive mitochondrial contamination, cells with mitochondrial genes accounting for >30% of the total genes were discarded. Subsequently, t-distributed random neighborhood embedding (t-SNE) was applied to the 2D representation of data structures. After clustering, the Bausingler (version 1.2.4) package was used to identify the types of co-cultured cells. After obtaining the differentially expressed gene information of each cell group, functional analysis such as Gene Ontology (GO) pathway enrichment analysis, Kyoto Encyclopedia of Genes and Genomes (KEGG) set analysis, and functional prediction were performed using data from the CancerSEA database (http://biocc.hrbmu.edu.cn/CancerSEA/), which is a multifunctional website designed to comprehensively explore the different functional states of cancer cells at the single-cell level. R package (version 3.6.2) was used to process the raw scRNA-seq data, and Seurat package (version 3.1.4) was utilized to analyze the gene expression data.



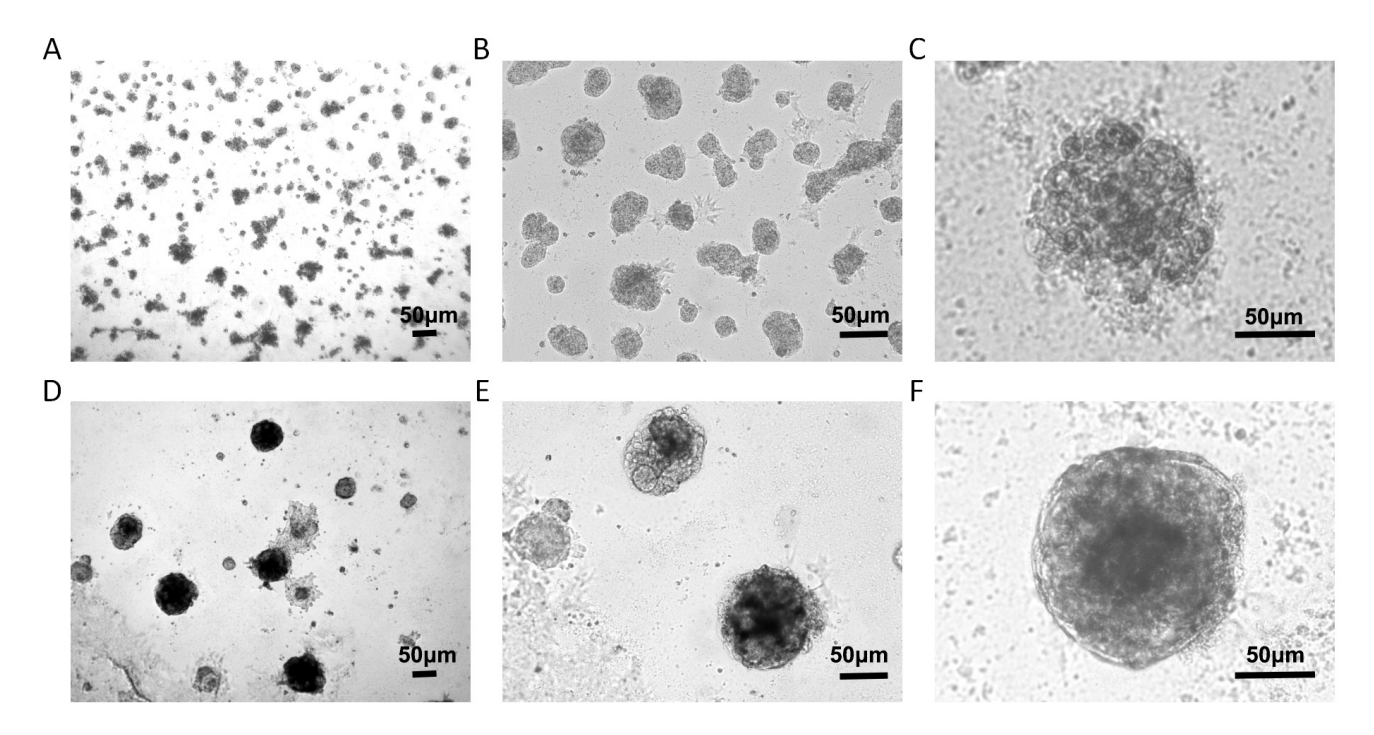


Fig. 1. Cell morphology in the 3D culture. (A–C) Individual MCF-7 cells in the 3D culture produced irregular cell spheres. (D–F) Three-dimensional co-culture model for MCF-7 cells, HMFs, and HUVECs formed 3D structures with smooth edges. Scale bar value: 50 μm. MCF, michigan Cancer Foundation; HMFs, human mammary fibroblasts; HUVECs, human umbilical vein endothelial cells.

2.4 RT-qPCR

Total RNA was extracted from MCF-7 cells in 3D culture group and 3D co-culture model group (see 2.1) using TRIzol (Invitrogen, Carlsbad, CA, USA). Then, RNA was aliquoted to synthesize cDNA using the Reverse Transcription System (Promega, Madison, WI, USA). Quantitative reverse transcriptase polymerase chain reaction (qRT-PCR) products were amplified using a SYBR green PCR Master Mix kit (Qiagen, Germantown, PA, USA) according to the manufacturer's instructions on the ABI Prism 7500 Detection System (Applied Biosystems, Carlsbad, CA, USA). Data were analyzed using the $2^{-\Delta\Delta Ct}$ method, and GAPDH was regarded as an internal control [13]. The following q-PCR primer sequences were used: S100P forward, 5'-GCACCATGACGGAACTAGAGACA-3', and reverse, 5'-CAGGTCCTTGAGCAATTTATCCAC-3'; HSPB1 forward, 5'-CTGACGGTCAAGACCAAGGATG-3', and reverse, 5'-GTGTATTTCCGCGTGAAGCACC-3'; COX6C forward, 5'-GTAGCATTCGTGCTATCCCTGG-3', and reverse, 5'-GATACCAGCCTTCCTCATCTCC-3'; CRABP2 forward, 5'-TTGAGGAGCAGACTGTGGATGG-3', and reverse, 5'-GTTCTCTGGTCCACGAGGTCTT-3'; SOD2 5'-CTGGACAAACCTCAGCCCTAAC-3', forward, and reverse, 5'-AACCTGAGCCTTGGACACCAAC-3'; GAPDH forward, 5'-GCACCGTCAAGGCTGAGAAC-3' and reverse, 5'-TGGTGAAGACGCCAGTGGA-3'. Analysis between two groups was performed using an unpaired Student's t-test.

3. Results

3.1 Cell Morphology in the 3D Culture

Two types of 3D culture were established. One was constructed for individual MCF-7 cell 3D culture. Under a microscope, it appeared messy, and it had a rough edge (Fig. 1A–C). The other was established for MCF-7 cells co-cultured with HMFs and HUVECs. The cell masses presented with a smoother and more regular edge (Fig. 1D–F).

3.2 Single-cell Transcriptome Sequencing Atlas and Cell Type Identification

After controlling the quality of single-cell analysis (Fig. 2A), dead or injured cells were eliminated. Eventually, we obtained 2041 cells in MCF-7 cells in the 3D culture, 1043 cells in MCF-7 cells in the 3D culture treated with cisplatin, 2421 cells in the 3D co-culture model, and 4667 cells in the 3D co-culture model with cisplatin. The cells of the 3D co-culture model (from the 3D co-culture model and 3D co-culture model with cisplatin) were clustered into six according to the hypervariable gene using the standard data analysis tool K-means in Seurat package (Fig. 2B). Next, the cells were visualized in the t-SNE map. The heatmap presented the expressions of the top 5 differentially expressed genes in each of the six cluster (Fig. 2C, Table 1). The differentially expressed genes were analyzed using the Kruskal-Wallis test in R package. The cell type was identified with marker genes and the characteristic genes of each cell type. The HUVECs, HMFs, and MCF-7 cells of the 3D co-culture model, which was shown



Table 1. Top 5 differentially expressed genes in each of the six cluster.

Clusters			Genes		
Cluster 1	IGFBP7	S100A6	PADI2	TGM2	IGFBP4
Cluster 2	HILPD4	MT1X	HIST1H2BG	ANKRD37	CCL20
Cluster 3	HLA-A	AL450405.1	NCCRP1	SRGN	S100A4
Cluster 4	TUBA1B	UBE2C	STMN1	HJURP	TOP2A
Cluster 5	TFF1	TXNIP	COX6C	CLSN4	DSCAM-AS1
Cluster 6	MMP2	COL6A1	<i>IGFBP5</i>	COL6A3	COL1A1

Table 2. Top 10 differentially expressed genes in HUVECs, MCF-7 cells, and HMFs.

Cells	Genes
HUVEC	C15orf48, PLAU, CCL20, PDZK1IP1, MT2A, ARL4C, SOD2, MT1X, CEBPB, SFN
MCF-7	TXNIP, COX6C, CRABP2, CCN5, S100P, CLDN4, AL450405.1, TFF1, KRT19, HLA-A
HMF	MMP2, COL6A1, SPARC, DCN, COL6A1, COL6A2, COL6A3, HLLA-C, LUM, IGHBP5

in the t-SNE map, were separated (Fig. 3A). Each cell type was featured individually in the sole t-SNE map (Fig. 3B-D). The heatmap depicted the expressions of the top 10 differentially expressed genes in HUVECs, MCF-7 cells, and HMFs (Fig. 2D, Table 2). Fig. 3E presents the characteristic genes of HUVECs including CCL20, MT2A, SOD2, MT1X, and CEBPB. In addition, the relative expressions of C15ORF48, PLAU, PDZK1IP1, and ARL4C in the three cell types were examined, as these genes had relatively high expression levels in HUVECs (Fig. 3E). Similarly, Fig. 3F depicts the characteristic genes of HMFs such as MMP2, SPARC, and COL1A1. In addition, the relative expressions of COL6A1, DCN, COL6A3, HLA-C, LUM, and IGFBP5 in the three cell types were examined, as these genes had a relatively high expression levels in HMFs (Fig. 3F). Further, Fig. 3G presents the characteristic genes of MCF-7 cells including TXNIP, COX6C, CRABP2, CCN5, CLDN4, TFF1, KRT19, and HLA-A. Fig. 3G shows the relative expressions of AL450405.1 in the three cell types, as it had a relatively high expression level in MCF-7 cells.

3.3 Single-cell RNA Sequencing of MCF-7 Cells in the 3D Co-culture Model Showed Differential Response to Cisplatin Compared with that of MCF-7 Cells in the 3D Culture

To further assess the 3D co-culture model, the function differentialGeneTest in R package was used to calculate the differentially expressed genes in each pairwise comparison. As shown in Fig. 4A, the heatmap presented the expressions of the top 20 differentially expressed genes in MCF-7 cells in the 3D culture and MCF-7 cells in the 3D co-culture model. Further, as shown in Fig. 4B, the heatmap depicted the expressions of the top 20 differentially expressed genes in MCF-7 cells in the 3D culture with cisplatin and MCF-7 cells in the 3D co-culture model with cisplatin. According to the two figures, they showed plenty of similarities. With or without cisplatin, the expressions of *SOD2*, *CEBPB*, *PLAU*, *SFN*, *IGFBP7*, *MT2A*, and *VIM* were relatively high in MCF-7 cells in the 3D culture but

relatively low in MCF-7 cells in the 3D co-culture model. Meanwhile, the expressions of S100P, ALDOC, HSPA1B, HSPB1, COX6C, CRABP2, TXNIP, and AQP3 were relatively low in MCF-7 cells in the 3D culture but relatively high in MCF-7 cells in the 3D co-culture model. RT-qPCR results demonstrated that SOD2 mRNA level was downregulated, while S100P, HSPB1, COX6C and CRABP2 mRNA expressions were upregulated in the 3D co-culture model in comparison to in the 3D culture alone (Supplementary Fig. 1A–E), which consistent to above analysis. As shown Fig. 4C, the heatmap depicted the expressions of the top 20 differentially expressed genes in MCF-7 cells in the 3D culture and MCF-7 cells in the 3D culture with cisplatin. Further, as depicted in Fig. 4D, the heatmap presented with the expressions of the top 20 differentially expressed genes in MCF-7 cells in the 3D co-culture model and MCF-7 cells in the 3D co-culture model with cisplatin. As shown in the two figures, regardless if the MCF-7 cells were co-cultured with other cells or not, the ZFP36 expressions were partially low in cells without cisplatin but relatively high in cells with cisplatin.

The bubble graph displayed the top 30 differential GO pathway enrichment between MCF-7 cells in the 3D culture and MCF-7 cells in the 3D co-culture model (Fig. 4E), including the pathways of focal adhesion, cell-substrate adherens junction, and cell-substrate junction. The bubble graph showed the top 30 differential GO pathway enrichment between MCF-7 cells in the 3D culture with cisplatin and MCF-7 cells in the 3D co-culture model with cisplatin (Fig. 4F), including focal adhesion, cell-substrate adherens junction, and cell-substrate junction.

3.4 Functional Correlation Analysis of Differentially Expressed Genes between MCF-7 Cells in the 3D Co-culture Model and MCF-7 Cells in the 3D Co-culture Model with Cisplatin from the CancerSEA Website

The differentially expressed genes between MCF-7 cells in the 3D co-culture model and MCF-7 cells in the 3D co-culture model with cisplatin were uploaded to fur-



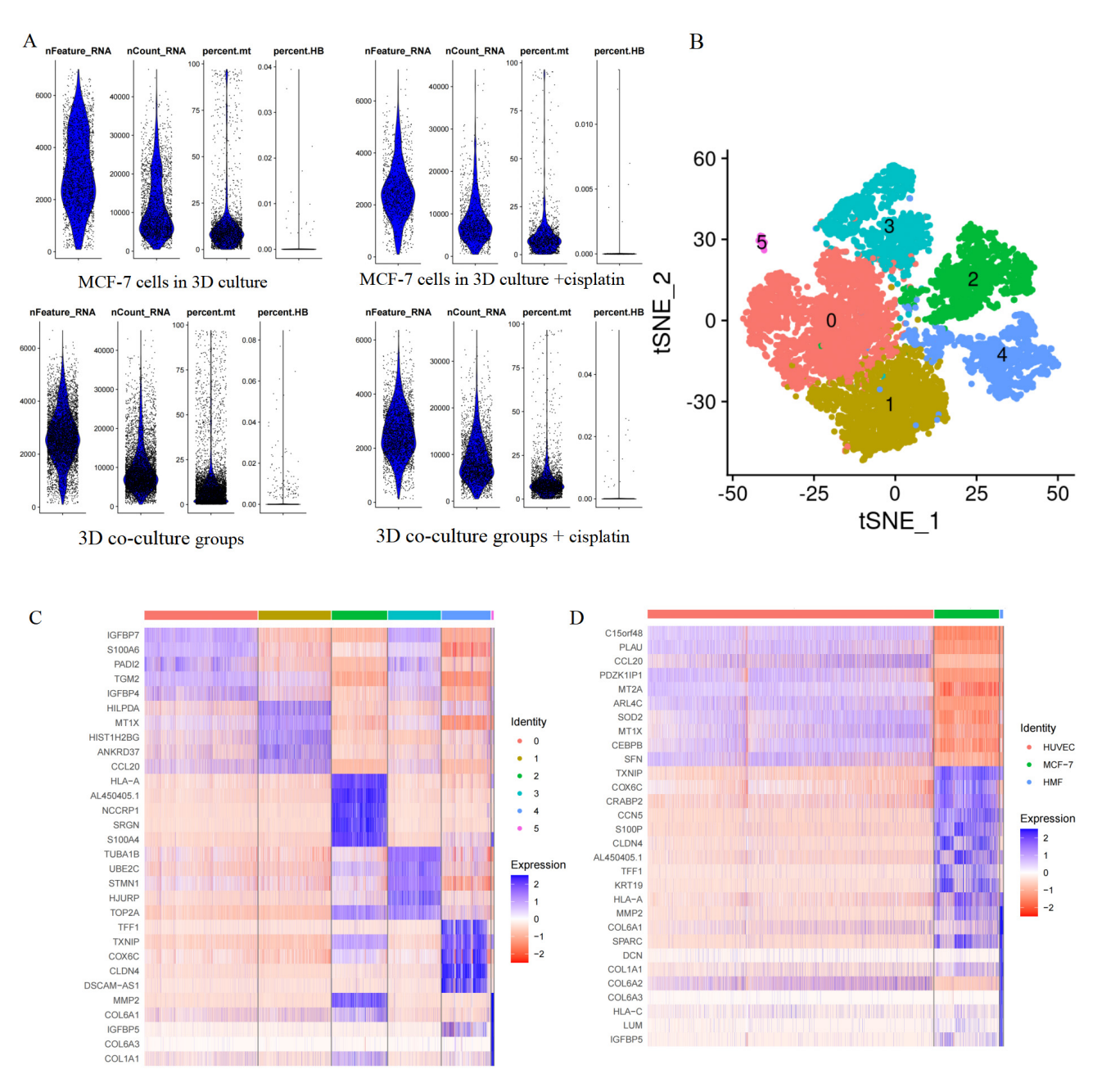


Fig. 2. Cell cluster and single-cell transcriptome sequencing atlas. (A) Quality control for scRNA-seq. Violin plot of nFeature_RNA presented the number of genes captured in a sample cell. Violin plot of nCount_RNA presented the number of the total number of genes expressed in the cells. Violin plot of percent.mt presented the mitochondrial gene expression ratio. Violin plot of the erythrocyte gene expression ratio. (B) Cells of the 3D co-culture model were clustered into six. (C) The heatmap showed the expressions of the top 10 differentially expressed genes in each of the six clusters. (D) The heatmap showed the expressions of the top 10 differentially expressed genes in HUVECs, MCF-7 cells, and HMFs. scRNA-seq, single-cell RNA sequencing; tSNE, t-distributed Stochastic Neighbor Embedding; HUVECs, human umbilical vein endothelial cells; HMFs, human mammary fibroblasts.

ther understand the influence of the 3D co-culture model treated with cisplatin. The map explained the expression level of each differentially expressed gene in each breast cancer cell from the CancerSEA website database (Fig. 4G). Moreover, the heatmap performed the functional correlation analysis of differentially expressed genes between MCF-7 cells in the 3D co-culture model and MCF-7 cells

in the 3D co-culture model with cisplatin from four different datasets in the CancerSEA website, which include mechanisms such as apoptosis, DNA damage, hypoxia, and metastasis (Fig. 4H).



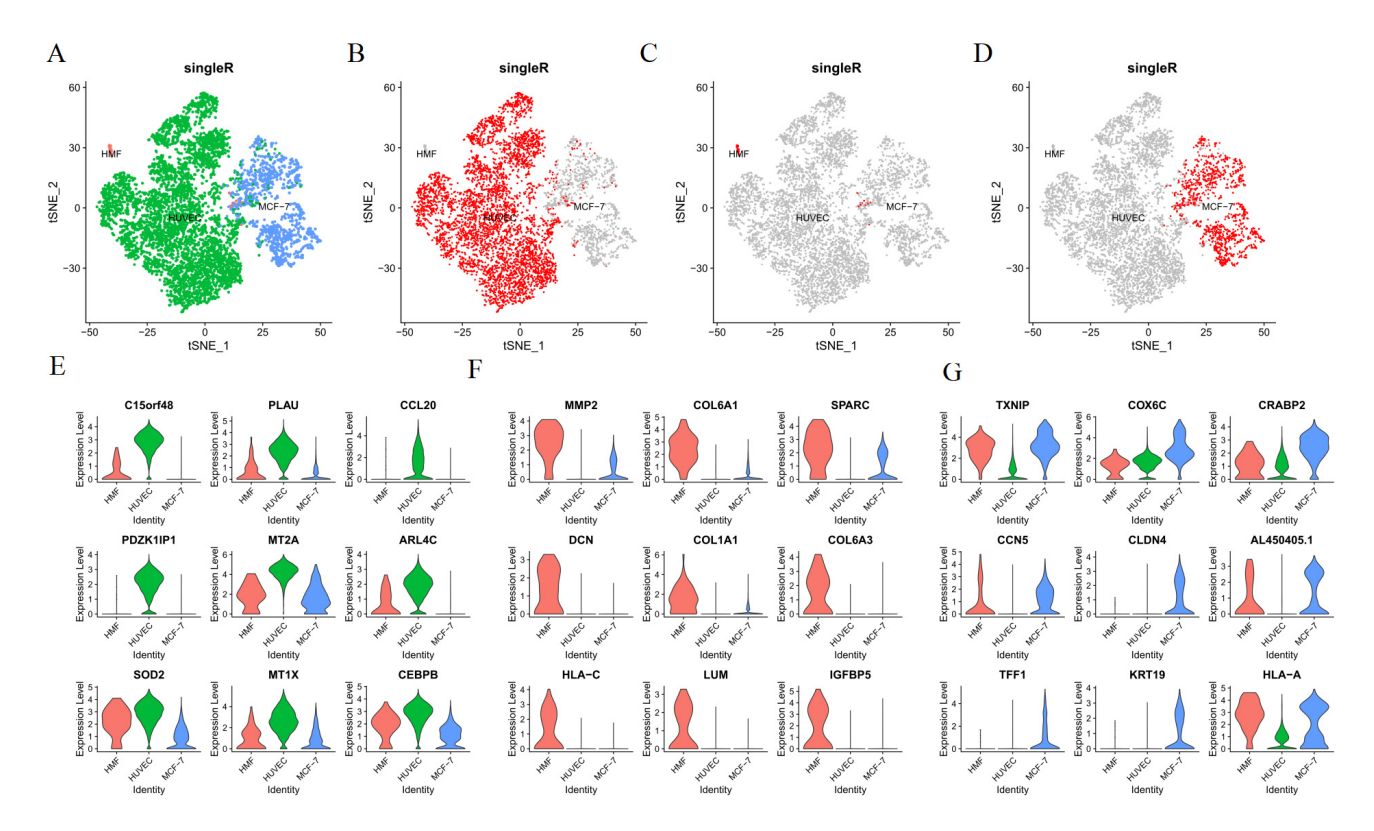


Fig. 3. Identification of cell types. (A) The map of the identification of all cells. (B–D) The map of distribution of HUVECs, HMFs, and MCF-7 cells. (E) The relative expressions of the characteristic genes of HUVECs. (F) The relative expressions of the characteristic genes of MCF-7 cells.

4. Discussion

This study showed that MCF-7 cell clusters in the 3D co-culture model had smoother edges compared with those in the mono-cultured model. Single-cell RNA analysis revealed that the expression of *SOD2* was low. Meanwhile, the expression of *S100P*, *HSPB1*, *COX6C*, and *CRABP2* in MCF-7 cells in the 3D co-culture model was higher than that in MCF-7 cells in the 3D mono-culture model. Functional enrichment analysis showed that differentially expressed genes between the 3D co-culture group and the 3D co-culture group with cisplatin were enriched in the pathways associated with apoptosis, DNA damage, hypoxia, and metastasis.

This study aimed to improve the traditional cell coculture technique using the single-cell sequencing technology to mimic the real environment *in vivo*. Currently, the generic 3D *in vitro* culture models used for scientific and preclinical studies comprise a single type of cells [14]. In contrast, the interactions between tumors and the stroma and cells remain complex, and they are still not identified and, thus, should not be disregarded. With advancements in the manufacturing technology, more biomaterials can be used to construct 3D culture models that mimic the internal microenvironment of tumors [15]. Collagen, sodium alginate, hyaluronic acid, sericin, and gelatin have been used to construct 3D breast cancer models [16,17]. Corning matrix gel is a natural extracellular matrix-based hydrogel containing laminin, type IV collagen, acetyl heparan sulfate proteoglycan, pentosan/nestin, and various growth factors, which are widely suitable for *in vitro* 3D culture [18]. If direct *in vitro* 3D culture is performed with scRNA-seq, it will be more relevant to evaluate the pathogenesis of different tumors including breast lesions or conduct studies such as those on clinical drug sensitivity screening.

With single-cell sequencing, three types of co-cultured cells were isolated, and more cells could be assessed. The environment in which tumor cells invaded the body at the time of onset was considered. A recent report revealed that with surrounding HMFs, fibroblasts may modulate endoplasmic reticulum (ER) signaling in MCF-7 cells to decrease apoptosis [19]. Several studies on 2D co-culture with HUVECs and MCF-7 cells revealed that MCF-7 cells can promote HUVECs under specific conditions [20,21]. Hence, a 3D co-culture model containing HUVECs, HMFs, and MCF-7 cells, which has never been reported until now, was constructed. The edges of cell masses of MCF-7 cells co-cultured with HUVECs and HMFs were smoother than that of MCF-7 cells cultured individually. This may be attributed to the various sizes of the three types of cells, which makes it easier for their intercellular spaces to fuse with each other when forming a cell mass.

As shown in Fig. 4A,B, co-culture influenced the expressions of marker genes in MCF-7 cells. The overexpres-



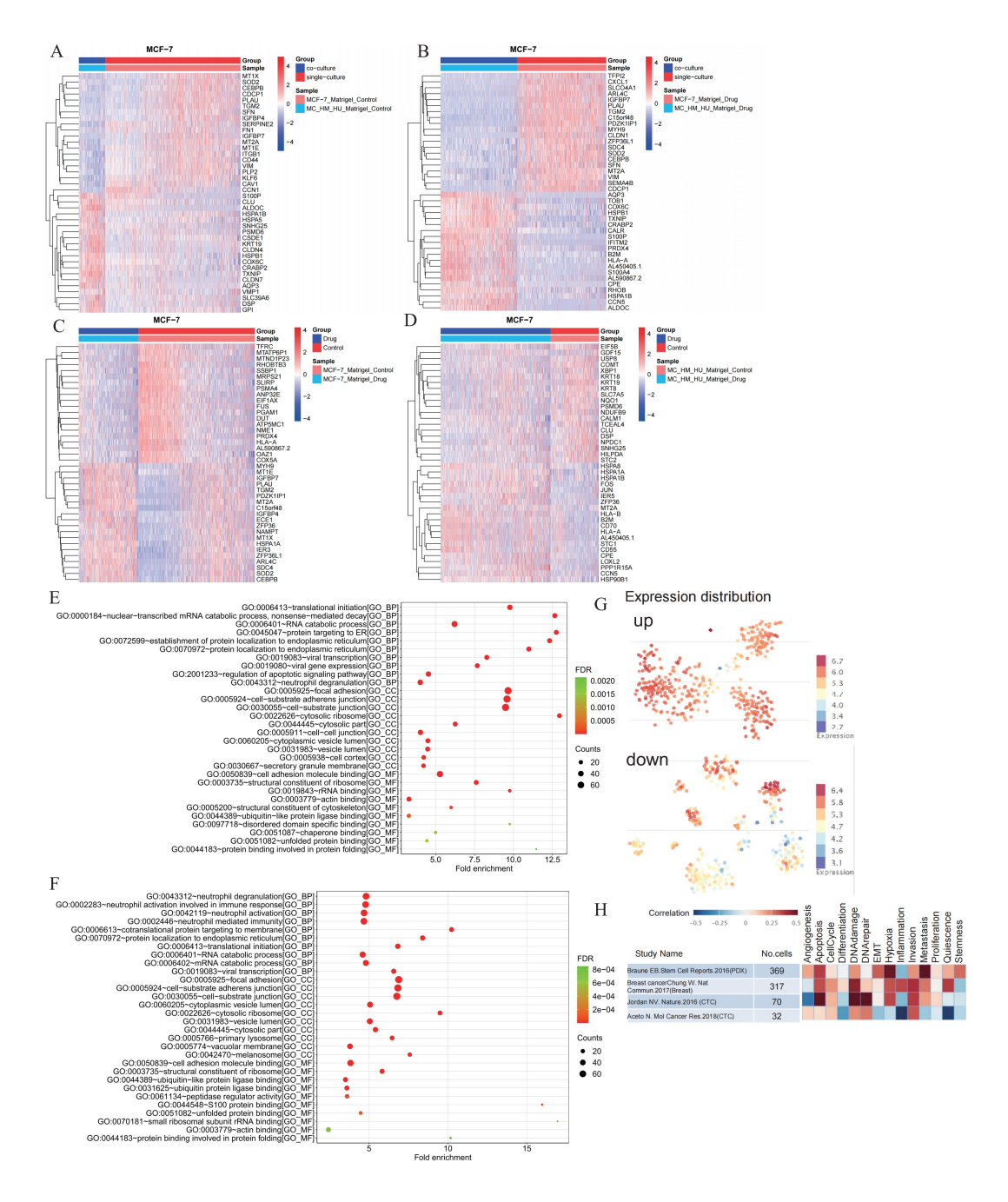


Fig. 4. Analysis of differentially expressed genes and GO pathway enrichment based on single-cell RNA sequencing in MCF-7 cells. (A) The heatmap showed the expressions of the top 20 differentially expressed genes in MCF-7 cells in the 3D co-culture model. (B) The heatmap showed the expressions of the top 20 differentially expressed genes in MCF-7 cells in the 3D culture with cisplatin and MCF-7 cells in the 3D co-culture model with cisplatin. (C) The heatmap showed the expressions of the top 20 differentially expressed genes in MCF-7 cells in the 3D culture and MCF-7 cells in the 3D culture with cisplatin. (D) The heatmap showed the expressions of the top 20 differentially expressed genes in MCF-7 cells in the 3D co-culture model and MCF-7 cells in the 3D. (E) GO pathway enrichment between MCF-7 cells in the 3D culture and MCF-7 cells in the 3D co-culture model. (F) GO pathway enrichment between MCF-7 cells in the 3D culture with cisplatin and MCF-7 cells in the 3D co-culture model with cisplatin. (G) Expression level of each differentially expressed gene in each breast cancer cell from the CancerSEA website database. (H) Functional correlation analysis was performed for differentially expressed genes of MCF-7 cells in 3D co-culture models and MCF-7 cells in 3D co-culture models of cisplatin from 4 different datasets of CancerSEA website. GO, Gene Ontology; TME, tumor microenvironment. FDR, false discovery rate



sion of SOD2 in MCF-7 cells may decrease cell death [22], and the SOD2 expression can be low in the 3D co-culture model. S100P suppressed the cytotoxicity of IFN- β to MCF-7 cells [23], and the expression of S100P was higher in MCF-7 cells in the 3D co-culture model than in MCF-7 cells in the 3D mono-culture model. Due to the overexpression of HSPB1 and COX6C in MCF-7 cells, tumors can be less sensitive to chemotherapy and radiotherapy [24,25]. Thus, the expression of HSPB1 and COX6C was higher in MCF-7 cells in the 3D co-culture model than in MCF-7 cells in the 3D mono-culture model. This finding is consistent with that of previous studies showing that 3D-cultured cells can reduce drug sensitivity [26–28]. CRABP2 inhibits breast cancer cells [29], and the expression of CRABP2 was high in the 3D co-culture model. A previous study showed that Aquaporin 3 (AQP3), which had a high expression in the 3D co-culture model, could promote the effect of 5'-DFUR and gemcitabine, but not that of cisplatin, against breast cancer cells [30]. The 3D co-culture model built with HUVECs, HMFs, and MCF-7 cells was found to be an effective 3D co-culture model for breast cancer. According to our results, with GO pathway enrichment, the most typical differential pathways involving focal adhesion, cellsubstrate adherens junction, and cell-substrate junction may be attributed to the fact that the Matrigel matrix contains viscosifier. Hence, cells can have an increased expressions of adhesion molecules. In addition, the CancerSEA website plays an extensive role in our research. Moreover, it can provide an important reminder regarding the importance of evaluating the correlation between apoptosis, DNA damage, hypoxia, and metastasis as well as our 3D co-culture model.

The current study had several limitations. That is, co-culture cell types did not use immune cells, and there were also differences in the actual biological environment *in vivo*. Therefore, changes that occur in cell types other than breast cancer cells after cisplatin treatment and the effects of cisplatin treatment on the interactions between different cell types should be analyzed. In addition, the proportion of HMF was relatively low at the end of the experiment, and the proportion of cells used in constructing cell co-culture models must be further optimized.

5. Conclusion

A novel 3D co-culture model of breast cancer was successfully constructed based on the single-cell RNA sequencing technology. Results revealed that the experimental results met the expected scientific properties. According to our experimental method, there was a significant improvement in the traditional cell experimental method, which can be recommended for drug development or drug resistance research and used for general experimental research on cell–cell interactions.

Availability of Data and Materials

The datasets used and/or analyzed during the current study are available from the corresponding author on reasonable request.

Author Contributions

DZ and WLi conceived and designed the experiments. WLuo, PXC, and SQY performed the experiments. KRL, TCH and XFM analyzed the data. HQH searched the literature. GYY, GLY, and AGW draw charts. GYY and DZ drafted, proofread and revised the manuscript. All authors contributed to editorial changes in the manuscript. All authors read and approved the final manuscript. All authors have participated sufficiently in the work and agreed to be accountable for all aspects of the work.

Ethics Approval and Consent to Participate

Not applicable.

Acknowledgment

The authors want to thank Guangzhou GenCoding Co., Ltd. and Guangzhou ASD Biomedical Tech Co., Ltd. for their technical support in this study.

Funding

This work was supported by the Guangdong Medical Research Fund (grant number: A2019329), and Foshan 14th Five-Year High-Level Key Specialty Construction Project.

Conflict of Interest

The authors declare no conflict of interest.

Other Declarations

This manuscript was submitted as a pre-print at https://www.researchsquare.com/article/rs-634121/v1.

Supplementary Material

Supplementary material associated with this article can be found, in the online version, at https://doi.org/10.31083/j.fbl2912406.

References

- [1] Vis MAM, Ito K, Hofmann S. Impact of Culture Medium on Cellular Interactions in *in vitro* Co-culture Systems. Frontiers in Bioengineering and Biotechnology. 2020; 8: 911. https://doi.org/10.3389/fbioe.2020.00911
- [2] Thayanithy V, O'Hare P, Wong P, Zhao X, Steer CJ, Subramanian S, et al. A transwell assay that excludes exosomes for assessment of tunneling nanotube-mediated intercellular communication. Cell Communication and Signaling: CCS. 2017; 15: 46. https://doi.org/10.1186/s12964-017-0201-2
- [3] Chaicharoenaudomrung N, Kunhorm P, Noisa P. Threedimensional cell culture systems as an *in vitro* platform for can-



- cer and stem cell modeling. World Journal of Stem Cells. 2019; 11: 1065–1083. https://doi.org/10.4252/wjsc.v11.i12.1065
- [4] Ziółkowska-Suchanek I. Mimicking Tumor Hypoxia in Non-Small Cell Lung Cancer Employing Three-Dimensional In Vitro Models. Cells. 2021; 10: 141. https://doi.org/10.3390/ce lls10010141
- [5] Langhans SA. Three-Dimensional in Vitro Cell Culture Models in Drug Discovery and Drug Repositioning. Frontiers in Pharmacology. 2018; 9: 6. https://doi.org/10.3389/fphar.2018.00006
- [6] Tatara T, Mukohara T, Tanaka R, Shimono Y, Funakoshi Y, Imamura Y, et al. 3D Culture Represents Apoptosis Induced by Trastuzumab Better than 2D Monolayer Culture. Anticancer Research. 2018; 38: 2831–2839. https://doi.org/10.21873/anticanres.12528
- [7] Lugert S, Unterweger H, Mühlberger M, Janko C, Draack S, Ludwig F, et al. Cellular effects of paclitaxel-loaded iron oxide nanoparticles on breast cancer using different 2D and 3D cell culture models. International Journal of Nanomedicine. 2018; 14: 161–180. https://doi.org/10.2147/IJN.S187886
- [8] Fuzer AM, Lee SY, Mott JD, Cominetti MR. [10]-Gingerol Reverts Malignant Phenotype of Breast Cancer Cells in 3D Culture. Journal of cellular biochemistry. 2017; 118: 2693–2699.
- [9] Chen YC, Jung S, Zhang Z, Wicha MS, Yoon E. Co-culture of functionally enriched cancer stem-like cells and cancerassociated fibroblasts for single-cell whole transcriptome analysis. Integrative Biology: Quantitative Biosciences from Nano to Macro. 2019; 11: 353–361. https://doi.org/10.1093/intbio/zyz 029
- [10] Li F, Zhang H, Huang Y, Li D, Zheng Z, Xie K, et al. Single-cell transcriptome analysis reveals the association between histone lactylation and cisplatin resistance in bladder cancer. Drug Resistance Updates: Reviews and Commentaries in Antimicrobial and Anticancer Chemotherapy. 2024; 73: 101059. https://doi.org/10.1016/j.drup.2024.101059
- [11] Qin S, Jiang J, Lu Y, Nice EC, Huang C, Zhang J, *et al.* Emerging role of tumor cell plasticity in modifying therapeutic response. Signal Transduction and Targeted Therapy. 2020; 5: 228. https://doi.org/10.1038/s41392-020-00313-5
- [12] Du Z, Yang S, Gong Q, Lin Z, Xiao G, Mi S. Research of restricted migration evaluation of MDA-MB-231 cells in 2D and 3D co-culture models. Experimental Biology and Medicine (Maywood, N.J.). 2023; 248: 2219–2226. https://doi.org/10. 1177/15353702231214269
- [13] Sindhuja S, Amuthalakshmi S, Nalini CN. A Review on PCR and POC-PCR A Boon in the Diagnosis of COVID-19. Current Pharmaceutical Analysis. 2022; 18: 745–764.
- [14] Liverani C, De Vita A, Minardi S, Kang Y, Mercatali L, Amadori D, et al. A biomimetic 3D model of hypoxia-driven cancer progression. Scientific Reports. 2019; 9: 12263. https://doi.org/10.1038/s41598-019-48701-4
- [15] Cavo M, Caria M, Pulsoni I, Beltrame F, Fato M, Scaglione S. A new cell-laden 3D Alginate-Matrigel hydrogel resembles human breast cancer cell malignant morphology, spread and invasion capability observed "in vivo". Scientific Reports. 2018; 8: 5333. https://doi.org/10.1038/s41598-018-23250-4
- [16] Wang Y, Mirza S, Wu S, Zeng J, Shi W, Band H, et al. 3D hydrogel breast cancer models for studying the effects of hypoxia on epithelial to mesenchymal transition. Oncotarget. 2018; 9: 32191–32203. https://doi.org/10.18632/oncotarget.25891
- [17] Subia B, Dey T, Sharma S, Kundu SC. Target specific delivery of anticancer drug in silk fibroin based 3D distribution model of bone-breast cancer cells. ACS Applied Materials & Interfaces. 2015; 7: 2269–2279. https://doi.org/10.1021/am506094c
- [18] Lee HJ, Mun S, Pham DM, Kim P. Extracellular Matrix-Based

- Hydrogels to Tailoring Tumor Organoids. ACS Biomaterials Science & Engineering. 2021; 7: 4128–4135. https://doi.org/10.1021/acsbiomaterials.0c01801
- [19] Morgan MM, Livingston MK, Warrick JW, Stanek EM, Alarid ET, Beebe DJ, et al. Mammary fibroblasts reduce apoptosis and speed estrogen-induced hyperplasia in an organotypic MCF7-derived duct model. Scientific Reports. 2018; 8: 7139. https://doi.org/10.1038/s41598-018-25461-1
- [20] Jabbari N, Nawaz M, Rezaie J. Bystander effects of ionizing radiation: conditioned media from X-ray irradiated MCF-7 cells increases the angiogenic ability of endothelial cells. Cell Communication and Signaling: CCS. 2019; 17: 165. https://doi.org/10.1186/s12964-019-0474-8
- [21] González-González A, González A, Alonso-González C, Menéndez-Menéndez J, Martínez-Campa C, Cos S. Complementary actions of melatonin on angiogenic factors, the angiopoietin/Tie2 axis and VEGF, in co cultures of human endothelial and breast cancer cells. Oncology Reports. 2018; 39: 433–441. https://doi.org/10.3892/or.2017.6070
- [22] Ma S, Fu X, Liu L, Liu Y, Feng H, Jiang H, et al. Iron-Dependent Autophagic Cell Death Induced by Radiation in MDA-MB-231 Breast Cancer Cells. Frontiers in Cell and Developmental Biology. 2021; 9: 723801. https://doi.org/10.3389/fcell.2021. 723801
- [23] Kazakov AS, Mayorov SA, Deryusheva EI, Avkhacheva NV, Denessiouk KA, Denesyuk AI, et al. Highly specific interaction of monomeric S100P protein with interferon beta. International Journal of Biological Macromolecules. 2020; 143: 633– 639. https://doi.org/10.1016/j.ijbiomac.2019.12.039
- [24] Daniel P, Halada P, Jelínek M, Balušíková K, Kovář J. Differentially Expressed Mitochondrial Proteins in Human MCF7 Breast Cancer Cells Resistant to Paclitaxel. International Journal of Molecular Sciences. 2019; 20: 2986. https://doi.org/10.3390/ijms20122986
- [25] Chang FW, Fan HC, Liu JM, Fan TP, Jing J, Yang CL, et al. Estrogen Enhances the Expression of the Multidrug Transporter Gene ABCG2-Increasing Drug Resistance of Breast Cancer Cells through Estrogen Receptors. International Journal of Molecular Sciences. 2017; 18: 163. https://doi.org/10.3390/ijms 18010163
- [26] Ata FK, Yalcin S. The Cisplatin, 5-fluorouracil, Irinotecan, and Gemcitabine Treatment in Resistant 2D and 3D Model Triple Negative Breast Cancer Cell Line: ABCG2 Expression Data. Anti-cancer Agents in Medicinal Chemistry. 2022; 22: 371–377. https://doi.org/10.2174/1871520621666210727105431
- [27] Muguruma M, Teraoka S, Miyahara K, Ueda A, Asaoka M, Okazaki M, *et al.* Differences in drug sensitivity between two-dimensional and three-dimensional culture systems in triple-negative breast cancer cell lines. Biochemical and Biophysical Research Communications. 2020; 533: 268–274. https://doi.org/10.1016/j.bbrc.2020.08.075
- [28] Gomes LR, Rocha CRR, Martins DJ, Fiore APZP, Kinker GS, Bruni-Cardoso A, et al. ATR mediates cisplatin resistance in 3D-cultured breast cancer cells via translesion DNA synthesis modulation. Cell Death & Disease. 2019; 10: 459. https://doi.org/10.1038/s41419-019-1689-8
- [29] Feng X, Zhang M, Wang B, Zhou C, Mu Y, Li J, et al. CRABP2 regulates invasion and metastasis of breast cancer through hippo pathway dependent on ER status. Journal of experimental & clinical cancer research: CR. 2019; 38: 361. https://doi.org/10. 1186/s13046-019-1345-2
- [30] Trigueros-Motos L, Pérez-Torras S, Casado FJ, Molina-Arcas M, Pastor-Anglada M. Aquaporin 3 (AQP3) participates in the cytotoxic response to nucleoside-derived drugs. BMC cancer. 2012; 12: 1–10.

